

Original Research Article

Aerodynamic Coefficients Computation for Fixed Wing Aircrafts Using DATCOM Software with Emphasis on Rudderless Flying-Wing UAVsSevda Rezazadeh Movahhed , Mohammad Ali Hamed^{1*} 

1-2- Department of Mechanical Engineering, University of Tabriz, Tabriz, Iran

ABSTRACT**Article History:**

Received: 24.May.2023

Revised: 21.November.2023

Accepted: 01.December2023

Keywords: Fixed-wing aircraft, flying-wing UAV, aerodynamic coefficients, DATCOM.

The fixed-wing unmanned aerial vehicles (UAVs) have gained significant attention across diverse civilian and military applications in recent years, where precision control, advanced maneuverability, and elevated stealth capabilities are paramount. To design a robust control system to enable different tracking and path-following purposes, it is desired to establish a precise aerodynamic model. The research introduces a straightforward approach for accurately computing aerodynamic coefficients, essential for deriving aerodynamic forces and moments, particularly focusing on the rudderless flying-wing UAV models. Utilizing Digital DATCOM software, the study outlines a procedure for calculating the requisite aerodynamic coefficients of fixed-wing aircrafts. The data input card is prepared based on the design and physical attributes of the rudderless flying-wing Freya UAV model and its associated airfoil structure. Through the utilization of the input card in DATCOM software, computations are performed to determine static longitudinal/lateral stability, dynamic stability, and control coefficients, along with their derivatives. Additionally, a 3D model is constructed. The ensuing output file is then imported into the MATLAB environment for comprehensive analysis and integration into dynamic modeling for the design of control systems. The open-loop and closed-loop system performance analysis based on the obtained aerodynamic coefficients, shows acceptable values in terms of control surfaces and flight dynamics variables in the category of small-sized rudderless flying-wing UAVs which proves the reliability of the obtained results.

DOI: [10.22034/jast.2023.398894.1152](https://doi.org/10.22034/jast.2023.398894.1152)

Introduction

Fixed-wing UAVs have gained growing applications in recent years, because of their considerable features in terms of efficient performance in different maneuvers, even when carrying payloads [1-3]. The desired tracking behavior for performing different maneuvers may be achieved only by designing a robust control system. Accordingly, an accurate aerodynamic model is essential in the control system design process [4, 5].

Obtaining the equations of motion and building the aerodynamic model based on the presented data by the UAV manufacturer is a fundamental step in control system design. The aerodynamic coefficients are used to calculate the stability derivatives of the aerodynamic forces and

moments [6]. The drag, side, and lift forces and also the pitch, roll, and yaw aerodynamic moments are related to flight parameters and states by associated aerodynamic coefficients and derivatives, which may be calculated by pre-processed real flight data, wind tunnel tests, computational fluid dynamic analysis, and other practical and semi-practical methods [7-12].

In preliminary design operations, fast and optimal estimation of aerodynamic coefficients is a prerequisite. Generally, the analysis of aerodynamic parameters involves wind tunnel tests or Computational Fluid Dynamics (CFD) software, but these methods are not suitable for small-sized aircrafts. Wind tunnel tests are expensive and time-consuming, and their results may not be accurate, especially in low Reynolds number flight conditions. CFD software analysis,

¹ Corresponding Author, Mohammad Ali Hamed, Assistant Professor, Email: ma.hamed@tabrizu.ac.ir

while commonly used, often requires extensive work in creating a 3D model mesh and is highly complicated and time-consuming [13, 14]. An alternative approach is the use of DATCOM, introduced by the US Air Force which allows for parameter calculation based on a vast flight database, providing aerodynamic coefficients for the specified parameters.

In this paper, step-by-step aerodynamic modeling with DATCOM software is introduced to calculate the aerodynamic coefficients. In summary, the airplane's physical dimensions and design parameters are fed into DATCOM software in an input data card file. The software calculates the aerodynamic coefficients and other parameters which are stored in an output file. A 3D representation is also provided for identifying the correct input card data. The output statistics are further imported into the MATLAB environment for aerodynamic modeling and control system design purposes.

Materials and Methods

DATCOM software was originally developed based on the United States Air Force stability and control DATCOM [15] for estimating aerodynamic parameters and flight analysis of fixed-wing aircrafts [16]. DATCOM+Pro is also an improved version [17] which allows to plot airplane coefficients and running a 3D 6-DOF flight dynamic model. The overall procedure of the DATCOM modeling method is shown in Fig 1.

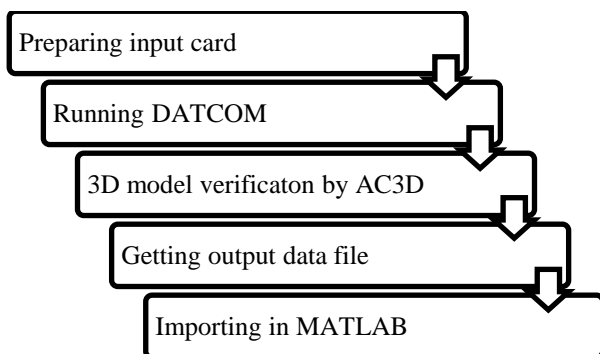


Fig 1. Overall process of the DATCOM method.

First of all, it is necessary to create the input data card (*.f, *.inp, *.dat) based on the geometrical body shape data, airfoil type, flight condition, and other information obtained from the manufacturer

data sheet with the structure defined in the next sections. The program starts by changing the input file extension to *.dcm and running it thereafter or calling the input card path address in DATCOM.exe software. A 3D model is demonstrated and an output file (*.out) is created in the same folder which contains the aerodynamic parameters estimated by DATCOM.

The output file may be used as an input in the MATLAB environment to carry out aerodynamic analysis, calculate the aerodynamic coefficients and derivatives, obtain aerodynamic forces and moments, and last but not least construct an aerodynamic model for a control system design. The modeling procedure by the proposed method is represented for a typical rudderless flying-wing UAV for better demonstration.

The rudderless flying-wing UAV is a fixed-wing type UAV equipped with elevons that play the role of elevators and ailerons simultaneously, the special design of which improves flight efficiency, stealth performance, structural strength, and integrity [18]. However, it faces challenges in designing a robust control system due to the lack of control surfaces and design characteristics. So, it is required to establish a comprehensive nonlinear aerodynamic model with accurate aerodynamic calculations [19]. The proposed procedure in this paper is implemented to get aerodynamic coefficients for the rudderless flying-wing UAV model demonstrated in Fig 2 (Freya, Smart Planes) [20-22].

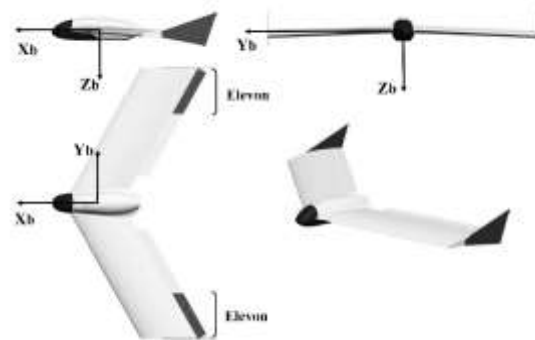


Fig 2. Schematic view of the Freya UAV [20].

2.1. Preparing data input card

The data input card must be prepared in a text or FORTRAN code file. An input card consists of many control cards and statements that form one or more cases. The name lists which are preceded by a "\$" sign (ex. \$FLTCN), are used to define the flight conditions and body shape dimensions.

The statements inside the name list are terminated with a "\$" sign. The main control cards and name lists used to create the input card structure are defined in the next subsections [16].

2.1.1. Command card

The command card is used to demonstrate different commands (Table 1).

Table 1. Command card.

Command	Definition
DIM	System of units
DAMP	Presence of the dynamic derivatives
DERIV	Dimension of the derivatives
PART	Provide auxiliary and partial outputs in each Mach number

The command DIM M shows that the dimensions must be in the metric unit system. Other unit systems are also available for analysis (DIM FT, DIM IN). A command card for the considered UAV model is presented in Fig 3. DERIV RAD also causes the static and dynamic derivatives to be measured in terms of radians.

```
*****
* List of Command Card *
*****
DIM M
DAMP
DERIV RAD
PART
```

Fig 3. Command card example.

2.1.2. Flight condition (FLTCON name list)

The name list \$FLTCON defines the flight conditions such as Mach number, vehicle weight, altitude, and values of the angle of attacks which are described in Table 2.

Table 2. FLTCON name list.

Variable	Definition
WT	Vehicle weight
NMACH	Number of the velocities to be run
MACH	Mach number
NALT	Number of atmospheric conditions or altitudes to be run
ALT	Altitude
NALPHA	Number of the angle of attacks to be tested
ALPHA	Angle of attack

Note that MACH, ALT, and ALPHA are arrays with NMACH, NALT, and NALPHA dimensions

respectively. FLTCON name list for the considered UAV model is represented in Fig 4.

```
*****
* Flight Conditions *
*****
$FLTCON WT=5.5701$

$FLTCON NMACH=1.0, MACH(1)=.04,
NALT=1.,ALT(1)=150.,
NALPHA=13.0,
ALSCHD(1)= -0.2, 0.0, 1.0, 2.0, 4.0, 6.0,
8.0, 10.0, 12.0, 14.0, 16.0, 18.0, 20.0$
```

Fig 4. FLTCON name list example.

2.1.3. Reference parameters (OPTINS name list)

The name list \$OPTINS describes the reference parameters such as wing area, wing span, and mean chord length (Table 3).

Table 3. OPTINS name list.

Variable	Definition
SREF	Wing area
CBARR	Mean chord
BLREF	Wing span

A typical input block for the OPTINS name list of the considered UAV model is presented in Fig 5.

```
*****
* Reference Parameters *
*****
$OPTINS BLREF=0.81, SREF=0.2712, CBARR=0.393$
```

Fig 5. OPTINS name list example.

Synthesis parameters (SYNTHS name list)

The \$SYNTHS name list defines the center of gravity, location of the wing, stabilizers, and fin (Table 4, Fig 6).

Table 4. SYNTHS name list.

Variable	Definition
XCG, ZCG	Center of gravity
XW, ZW	Location of the wing
XV, ZV	Location of the vertical stabilizer
XH, ZH	Location of the horizontal stabilizer
XVF, ZVF	Location of the fin
ALIW, ALIH	The incident angle for the wing and horizontal stabilizer
VERTUP	Vertical panel orientation

The location of the C.G., wing, or stabilizers is measured from an arbitrary datum axis which must be constant during all of the measurements. The command VERTUP=.TRUE. shows that the vertical stabilizer points up. Its value must change to FALSE if the vertical stabilizer has a downward configuration.

```
*****
* Group II      Synthesis Parameters *
*****
$SYNTHS XW=-0.015, ZW=0.0, ALIW=0.0, XCG=0.175, ZCG=0.00098,
ALIH=0.08
```

Fig 6. SYNTHS name list example.

Body configuration (BODY name list)

The \$BODY name list expresses the fuselage geometry (Table 5, Fig 7). Fuselage body cross-section may be circular, elliptical, or in other shapes. By defining the cross-section area S, DATCOM will calculate the radius and periphery. Other methods for defining the fuselage shape are also present [16].

Table 5. BODY name list.

Variable	Definition
NX, X	Number and location of the stations
S	Cross-section area of the fuselage
BLA	Length of cylindrical afterbody
BLN	Length of nose
BNOSE, BTAIL	Nose and tail shape parameters

X is a vector that shows the location of NX stations defined to enter fuselage characteristics such as area. The station locations are measured from the datum line. Note that, S is an array that gets the fuselage cross-section area calculated in each station; so, its dimension is NX. BNOSE and BTAIL values are set to 1.0 for conical type and set to 2.0 for sharp point type nose or tail.

```
*****
* Body Configuration Parameters *
*****
$BODY NX=6.,
BNOSE=1., BLN=0.0259, BLA=0.0367,
X(1)=-0.03, -0.02, 0.0, 0.45, 0.47, 0.48,
S(1)=.0, .0005, .001062, .001062, .0005, .05
```

Fig 7. BODY name list example.

Wing, horizontal tail, vertical tail, and vertical fin planform (PLNF name lists)

The name lists WGPLNF, HTPLNF, VTPLNF, and VFPLNF are included to describe wing, horizontal tail, vertical tail, and vertical fin planforms, respectively. The variables defined in Table 6 are identical for each surface considered, which are typically demonstrated for the wing planform in Fig 8 [17].

Table 6. PLNF name list.

Variable	Definition
CHRDR, CHRDT, CHRDBP	Airfoil chord at the root, and tip Chord length at the wing breakpoint
SSPN	Semi-span of the surface from the aircraft centerline to the tip.
SSPNE	Exposed distance from the fuselage to the tip
SAVSI, SAVSO	Sweep of the inboard, and outboard panels
DHDADI, DHDADO	Dihedral angles of the inboard, and outboard panels
TWISTA	Twist angle of the surface
TYPE	Planform type

Note that the root chord is measured from the centerline of the aircraft. The type of the surface defines TYPE value (straight tapered.1, Double delta. 2, Cranked. 3). As an example, the wing planform characteristics are given as the command card in Fig 9 for the considered UAV model.

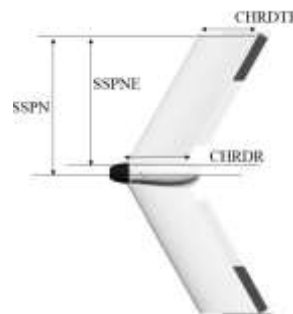


Fig 8. BODY variables of wing planform (WGPLNF) [17].

```
*****
* Wing planform variables *
*****
$WGPLNF CHRDR=0.45, CHRDT=0.33,
SSPN=0.405, SSPNE=0.355, TWISTA=-1.0, TYPE=1.,
SAVSI=27.41, DHDADI=0.5
NACA-W-4-0009
```

Fig 9. WGPLNF name list example.

The UAV model under study is a rudderless flying-wing UAV that lacks conventional horizontal and vertical stabilizers, so only WGPLNF is entered in the PLNF name list.

The NACA number denotes the airfoil type. The letters W, H, V, or F indicate wing, horizontal stabilizer, vertical stabilizer, or ventral fin respectively. The number denotes the series of the airfoil section. The wing airfoil of the Freya UAV falls into the 4-digit series NACA-0009 (Fig 10).



Fig 10. NACA-0009 airfoil [23].

2.1.7. Symmetric flaps (SYMFLP name list)

The input data for symmetrical control surfaces are described in \$SYMFLP name list, the variables of which are listed in Table 7.

Table 7. SYMFLP name list.

Variable	Definition
NDELTA, DELTA	Number of deflections, deflections
FTYPE	Type of flap
CHRDFI, CHRDFO	Chord of flap at the inboard, and onboard stations
SPANFI, SPANFO	Distance from the centerline for the inboard, and outboard edges of the flap surface

There are different types of symmetrical flaps (FTYPE=1. plain, 2. single slotted, 3. fowler, 4. double slotted, 5. split, 6. leading edge flaps, 7. Leading edge flaps, 8. Krueger). Elevators usually fall into plain-type symmetrical flaps, FTYPE=1.0. For example, the specification for elevons in the elevator role is given in Fig 11.

```
*****
*   ELEVATOR Deflection parameters   *
*****
$SYMFLP FTYPE=1.,NDELTA=9.,DELTA(1)=-12.,-9.,-6.,-3.,
0.,3.,6.,9.,12.,SPANFI=0.11,SPANFO=0.405,CHRDFI=0.05,
CHRDFO=0.05$
DERIV RAD
SAVE
CASEID ELEVATOR ANALYSIS, CASE 1
NEXT CASE
```

Fig 11. SYMFLP name list example.

Asymmetric flaps (ASYFLP name list)

The \$ASYFLP name list (Table 8) is used to define input data for asymmetric flaps which move in different directions to generate roll maneuvers. There are five flap types (STYPE=1. flap spoiler

on the wing, 2. plug spoiler on the wing, 3. spoiler-slot-deflection on the wing, 4. plain flap aileron, 5. differentially deflected moveable horizontal tail). The ailerons are usually defined by STYPE=4.0.

Table 8. ASYFLP name list.

Variable	Definition
NDELTA, DELTAL, DELTAR	Number of deflections, deflections of left, and right flaps
STYPE	Type of flap
CHRDFI, CHRDFO	Chord of flap at the inboard, and onboard stations
SPANFI, SPANFO	Distance from the centerline for the inboard, and outboard edges of the flap surface

Note that DELTAR and DELTAL should have opposite signs. The specifications contributing to elevons in the aileron role for Freya UAV are described in ASYFLP name list in Fig 12.

```
*****
*   AILERON Deflection parameters   *
*****
$ASYFLP STYPE=4.,NDELTA=9.,SPANFI=0.11,SPANFO=0.405,
CHRDFI=0.05,CHRDFO=0.05,DELTAL(1)=-12.,-9.,-6.,-3.,0.,
3.,6.,9.,12.,DELTAR(1)=12.,9.,6.,3.,0.,-3.,-6.,-9.,-12.$
DERIV RAD
CASEID AILERON ANALYSIS, CASE 1
NEXT CASE
```

Fig 12. ASYFLP name list example.

Running DATCOM, AC3D model

After preparing the input card in the correct format, the extension of the file is changed to *.dcm, or the input file path is called in the DATCOM software. By changing the file extension, DATCOM+PRO runs and a 3D model of the considered airplane is also demonstrated by the AC3Dview program which is used to verify whether the input data are given correctly and the desired aerial vehicle shape is established. The DATCOM.exe window after finalizing the calculations is shown in Fig 13.



Fig 13. DATCOM.exe window view.

Output file

After finishing the DATCOM analysis, the output file (*.out) containing calculated aerodynamic coefficients and other information, the 3D model (*.ac), and an XML file is created by which running, some valuable figures are generated automatically. Also, a *.csv file is provided which contains the output data in an excel format (The list of created output files is shown in Fig 14).

Name	Type
Freya.1.ac	ACID Model
Freya.2.ac	ACID Model
Freya.csv	Microsoft Excel Comma Separated Values File
Freya.xml	Datcom Input
Freya.lfi	LR plot data
Freya.out	DATCOM Output
Freya.xml	Extended Markup Language File
Freya_aero.xml	Extended Markup Language File

Fig 14. List of created output files.

The output file for the considered UAV model has the structure shown in Fig 15 which contains the calculated parameters for the given input card data.

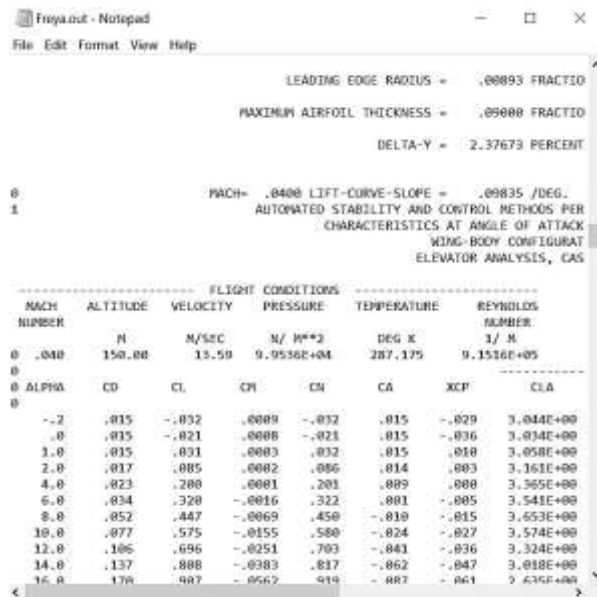


Fig 15. DATCOM output file (*.out).

Importing in MATLAB

Now, the calculated aerodynamic characteristics are called in MATLAB by the “datcomimport” command shown in the proper format in Fig 16. The output file (*.out) path address is given in parentheses.

```

aero=datcomimport('D:\freya.out',true,0);
data=aero(1);
    
```

Fig 16. Import output data in MATLAB.

Some missing aerodynamic coefficients ($C_{Y\beta}, C_{N\beta}, C_{lq}, C_{mq}$) are also called by the following command in Fig 17.

```

%% missing data
aerotab = ('cyb' 'cnb' 'clq' 'cmq');

for k = 1:length(aerotab)
    for m = 1:data.nmach
        for h = 1:data.nalt
            data.(aerotab(k))(1,m,h) = data.(aerotab(k))(1,m,h);
        end
    end
end
    
```

Fig 17. Importing missing data in MATLAB.

After importing the output data in MATLAB, the calculated aerodynamic coefficients are ready to use in aerodynamic calculations for dynamic modeling and further control system design purposes. For example, the data attributing to the drag aerodynamic coefficient C_d is listed by entering “data.cd” (Refer to MATLAB help for detailed information).

Simulation Results

DATCOM calculations

The DATCOM simulation results for the considered rudderless flying-wing Freya UAV [18, 20, 21] are presented in this section. The 3D model (Fig 18) is first provided which is in good accordance with the real UAV shape model.



Fig 18. AC3D model of Freya UAV.

By importing the data in MATLAB, the arrays of aerodynamic coefficients for Freya UAV are obtained in the defined angles of attacks. For example, the output longitudinal and lateral aerodynamic coefficients in the typical angle of attack $\alpha = 14 \text{ deg}$ are presented in Table 9. The desired mean or trim values may be also calculated based on the output data.

Table 9. Output aerodynamic coefficients for Freya UAV ($\alpha = 14 \text{ deg}$).

Long. aerodynamic coefficients	Value	Lat. aerodynamic coefficients	Value
C_{d0}	0.029	C_{Y0}	0
$C_{d\alpha}$	0.604	$C_{Y\beta}$	-0.0075
C_{dq}	0	C_{Yp}	0.1985
* $C_{d\delta e}$	0.0005	* $C_{Y\delta a}$	0.05
C_{l0}	0.2615	C_{L0}	0
$C_{l\alpha}$	3.0180	$C_{L\beta}$	-0.2804
C_{lq}	1.622	C_{Lp}	-0.2357
* $C_{l\delta e}$	0.7448	* $C_{L\delta a}$	0.1423
C_{M0}	0	C_{N0}	0
$C_{M\alpha}$	-0.4445	$C_{N\beta}$	-0.00105
C_{Mq}	-0.6147	C_{Np}	0.01685
* $C_{M\delta e}$	-0.3272	* $C_{N\delta a}$	-0.02976

* **Note:** the aerodynamic derivatives contributing to the control surfaces, are functions of control surface deflection and an average slope value is calculated.

Some representative figures plotted in MATLAB are demonstrated in Figs. (19-24). Note that by calculating the slope of the aerodynamic lift and moment coefficient with respect to the angle of attack α , the contributing aerodynamic coefficients $C_{l\alpha}$ and $C_{M\alpha}$ are obtained

respectively, which are comparable to aerodynamic derivatives already calculated by DATCOM (data.cla, data.cma).

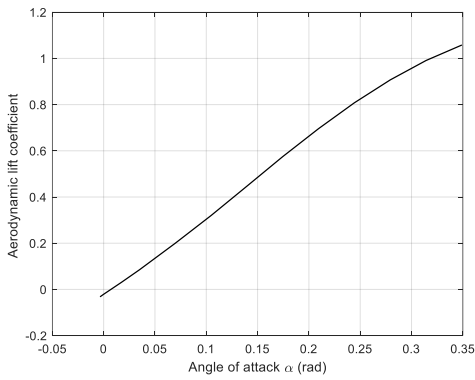


Fig 19. Aerodynamic lift coefficient C_l vs angle of attack α .

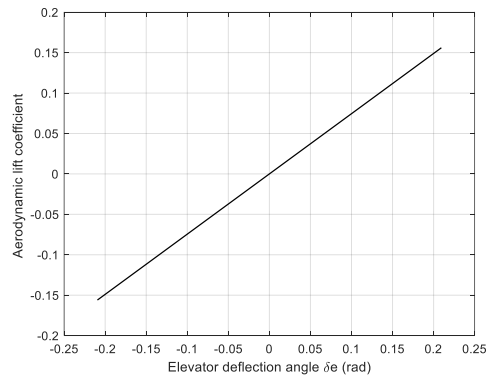


Fig 22. Aerodynamic lift coefficient C_l vs elevator deflection angle δ_e .

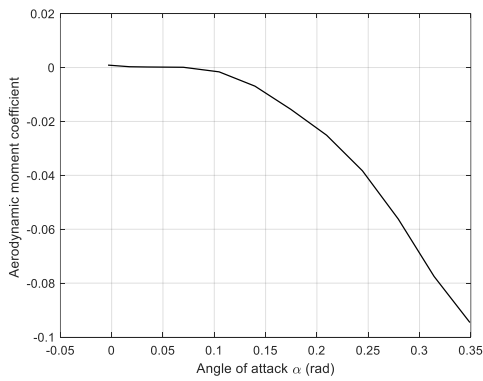


Fig 20. Aerodynamic moment coefficient C_M vs angle of attack α .

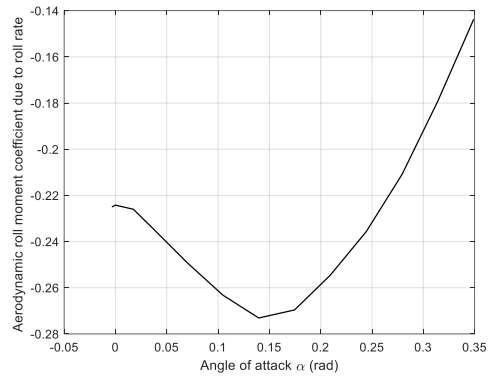


Fig 23. Aerodynamic roll moment coefficient due to roll rate C_{Lp} vs angle of attack α .

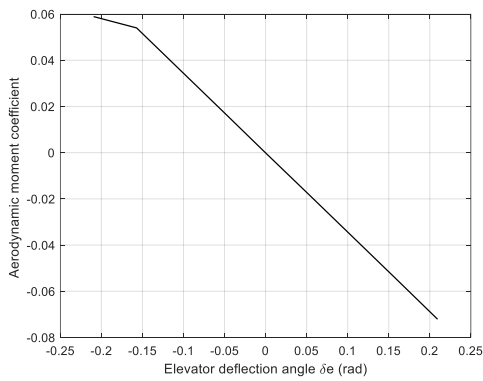


Fig 21. Aerodynamic moment coefficient C_M vs elevator deflection angle δ_e .

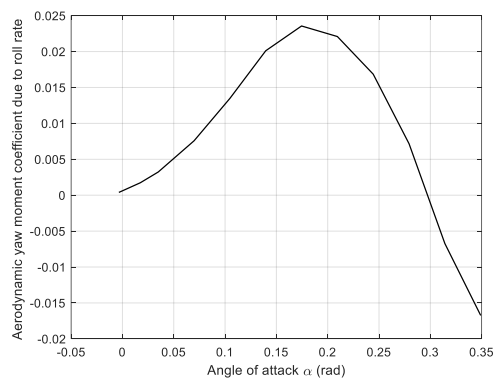


Fig 24. Aerodynamic yaw moment coefficient due to roll rate C_{Np} vs angle of attack α .

Some aerodynamic derivatives are not included directly in the output data file. For example, to obtain $C_{d\alpha}$, it is suggested to plot available drag

coefficient data C_d against the angle of attack, and calculate the slope of the figure using “polyfit” and “slope” commands in MATLAB by curve fitting (Fig 25). The results are compared to the figure provided by running XML file (Fig 26).

```
>> x = (data.alpha)*pi/180;
y1 = data.cd';
scatter(x,y1,'b','*');
P = polyfit(x,y1,1);
slope = P(1);
intercept = P(2);
yfit = P(1)*x+P(2); % P(1) is the slope and P(2) is the intercept.
hold on;

slope =

0.604317692602583
```

Fig 25. Obtaining aerodynamic drag derivative $C_{d\alpha}$ in MATLAB.

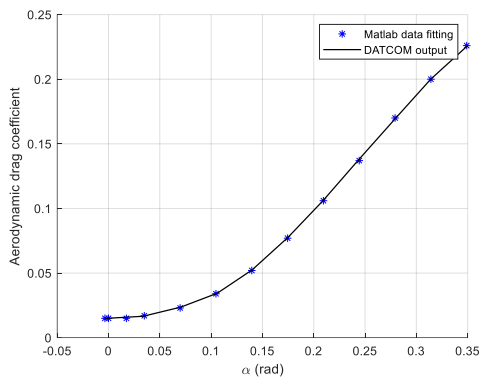


Fig 26. Aerodynamic drag coefficient C_d vs angle of attack α .

3.2 Stabilized closed-loop system performance

In this section, we examine the stability performance of the presumed Freya UAV through the implementation of a sliding mode control system with integral action featured with the optimization of the sliding surface design, as addressed by the methodology in [18]. It should be noted that according to the governing equations of motion, the UAV model under consideration shows dynamic instability in both longitudinal and lateral channels which is the characteristic of the considered UAV type. Furthermore, the flying-wing UAV without a rudder under investigation is equipped only with elevon control surfaces, lacking horizontal and vertical stabilizers and their associated control surfaces. Elevons function as elevators (δ_e) when moving in the same direction

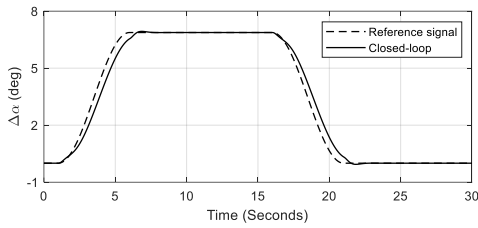
and as ailerons (δ_a) when moving in the opposite direction [4, 18]. The tracking performance of the UAV in longitudinal and lateral motions is assessed based on aerodynamic properties derived from the DATCOM software, as detailed in the preceding section of this paper.

Longitudinal motion dynamics result from aerodynamic forces and moments in the body plane $x_b - z_b$. The control inputs for this analysis include the engine throttle (δ_t) and elevator deflection (δ_e). The primary state variables influencing longitudinal motion are the angle of attack (α) and altitude (h).

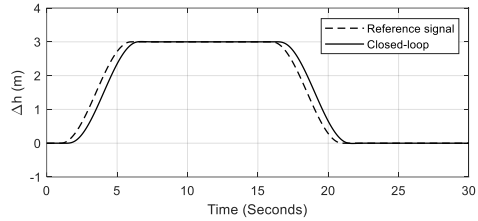
Figure 27 illustrates the tracking behavior of the angle of attack and altitude variation around the trim point. The chosen reference signal prompts the UAV to pitch up by approximately 7 degrees (0.12 radians) in the angle of attack and ascend by 3 meters, maintaining this configuration for 10 seconds before smoothly returning to its initial state and sustaining level flight.

Analysis of Figure 27 indicates that the system is dynamically stabilized, ensuring efficient tracking behavior within a finite time. The tracking error between the system output and desired values is negligible, and there is no significant overshoot in the system response. Moreover, the settling time is minimal, below one second, and no substantial delay in system response is observed. This approach is designed based on a precise dynamic system, relying on reliable aerodynamic calculations obtained through the proposed DATCOM methodology.

Figure 28 depicts the variation in control surface angle and engine thrust rate resulting from the considered control strategy, enforcing the system to track the desired trajectory, which are in the acceptable functioning range.

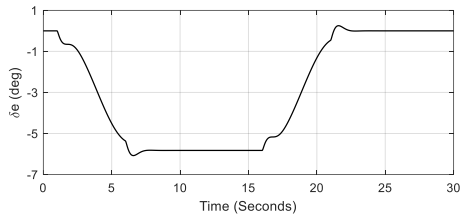


(a)

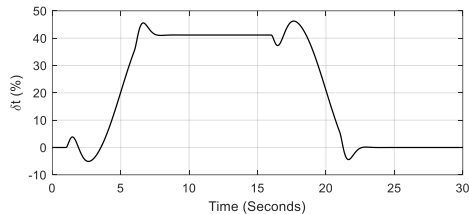


(b)

Fig 27. Tracking behavior about the trim point in longitudinal motion. (a) angle of attack variation $\Delta\alpha$ (deg), and (b) altitude variation Δh (m).



(a)



(b)

Fig 28. Control inputs in longitudinal motion. (a) elevator angle δ_e (deg), and (b) engine thrust rate δ_t (%).

Applying a similar control structure in lateral dynamics, leads to appropriate results in terms of flight stability and tracking performance. In lateral motion, the yaw angle (ψ) is managed to establish the direction of the UAV or maintain its straight trajectory. As previously noted, the UAV being investigated is a flying-wing design lacking vertical and horizontal stabilizers and their associated control surfaces. This implies that solely one control input i.e. aileron deflection (δ_a) affects the lateral dynamics. Figures (29, 30) demonstrate

the yaw angle variation tracking performance and aileron control surface respectively.

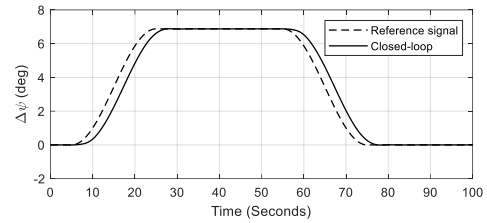


Fig 29. Tracking behavior about the trim point in lateral motion, yaw angle variation $\Delta\psi$ (deg).

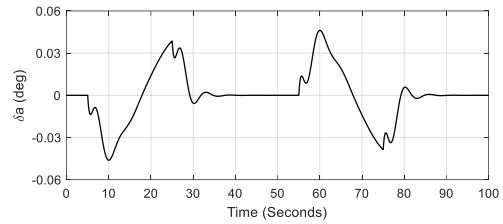


Fig 30. Control input in lateral motion, aileron angle δ_a (deg).

Conclusion

An accurate and straightforward approach for the calculation of aerodynamic coefficients based on DATCOM software is presented which is essential in any aerodynamic model design process. In this paper, step-by-step aerodynamic modeling is presented to calculate the aerodynamic coefficients using DATCOM software with a special focus on rudderless flying-wing UAVs. In summary, an input card for the DATCOM software is prepared using the physical characteristics and flight conditions of the rudderless flying-wing Freya UAV model. The aerodynamic coefficients and other parameters are calculated and stored in an output file. Using the DATCOM+PRO software, a 3D representation, an Excel file containing the output data, and an XML file is also created which are useful in aerodynamic modeling. The output statistics are further imported into MATLAB for aerodynamic analysis and control system design purposes. The assessment of open-loop and closed-loop system performance, utilizing the acquired aerodynamic coefficients, indicates satisfactory results concerning control surface deflections and flight dynamic variables within the small-sized flying-wing UAV category, which verifies the reliability of the results obtained.

Conflict of Interest

The authors of this paper declared no conflict of interest regarding the authorship or publication of this article.

References

- [1] P. Fahlstrom and T. Gleason, *Introduction to UAV systems*. John Wiley & Sons, 2012.
- [2] K. P. Valavanis and G. J. Vachtsevanos, *Handbook of unmanned aerial vehicles*. Springer, 2015.
- [3] P. Mátyás and N. Máté, "Brief history of UAV development," *Repüléstudományi Közlemények*, vol. 31, no. 1, pp. 155–166, 2019.
- [4] R. W. Beard and T. W. McLain, *Small unmanned aircraft*. Princeton university press, 2012.
- [5] B. Etkin and L. Reid, *Dynamics of Flight-Stability and Control, 3-th ed.* John Wiley & Sons, Inc., New York, 1994.
- [6] M. Cook, *Flight Dynamics Principles: A Linear Systems Approach to Aircraft Stability and Control*. Butterworth-Heinemann, 2013.
- [7] M. M. Londono, "Determination of Stability and Control Derivatives for a Modern Light Composite Twin Engine Airplane," 2009.
- [8] A. Rauf, M. A. Zafar, Z. Ashraf, and H. Akhtar, "Aerodynamic modeling and State-Space model extraction of a UAV using DATCOM and Simulink," in *2011 3rd International Conference on Computer Research and Development*, 2011, vol. 4: IEEE, pp. 88–92.
- [9] B. A. Siddiqui, "Reconfigurable flight control for high angle of attack fighter aircraft, with wind tunnel study," King Fahd University of Petroleum and Minerals (Saudi Arabia), 2010.
- [10] J. Shen, Y. Su, Q. Liang, and X. Zhu, "Calculation and identification of the aerodynamic parameters for small-scaled fixed-wing UAVs," *Sensors*, vol. 18, no. 1, p. 206, 2018.
- [11] D. Yang, J. Zang, J. Liu, and K. Liu, "Time-Domain Identification Method Based on Data-Driven Intelligent Correction of Aerodynamic Parameters of Fixed-Wing UAV," *Drones*, vol. 7, no. 9, p. 594, 2023.
- [12] Z. Hui and G. Chen, "Aerodynamic Parameter Estimation for a Morphing Unmanned Aerial Vehicle from Flight Tests," *Journal of Aerospace Information Systems*, vol. 20, no. 9, pp. 588–595, 2023.
- [13] P. Marqués and A. Da Ronch, *Advanced UAV aerodynamics, flight stability and control: novel concepts, theory and applications*. John Wiley & Sons, 2017.
- [14] B. M. Simmons, J. L. Gresham, and C. A. Woolsey, "Flight-Test System Identification Techniques and Applications for Small, Low-Cost, Fixed-Wing Aircraft," *Journal of Aircraft*, pp. 1–19, 2023.
- [15] D. Hoak and J. Carlson, "USAF Stability and Control DATCOM, Air Force Flight Dynamics Laboratory," *Ohio: Wright-Patterson Air Force Base*, 1978.
- [16] J. E. Williams and S. R. Vukelich, "The USAF stability and control digital DATCOM. Volume I. Users manual," MCDONNELL DOUGLAS ASTRONAUTICS CO ST LOUIS MO, 1979.
- [17] "http://www.holycows.net/datcom/Downloads/Datcom_Pro_Users_Manual_3.5.pdf".
- [18] S. R. Movahhed and M. A. Hamed, "Output tracking of a 6-DOF flying wing UAV in longitudinal motion using LQR optimized sliding mode control with integral action," in *2021 7th International Conference on Control, Instrumentation and Automation (ICCIA)*, 2021: IEEE, pp. 1–5.
- [19] R. C. Nelson, *Flight stability and automatic control*. WCB/McGraw Hill, New York, 1998.
- [20] S. Bagheri, "Modeling, simulation and control system design for civil unmanned aerial vehicle (uav)," Umea University, 2014.
- [21] S. Bagheri, T. Jafarov, L. Freidovich, and N. Sepehri, "Beneficially combining LQR and PID to control longitudinal dynamics of a SmartFly UAV," in *7th IEMCON*, 2016: IEEE, pp. 1–6.
- [22] "<https://www.Smartplanes.com>".
- [23] "<https://www.ntrs.nasa.gov>".

COPYRIGHTS

©2024 by the authors. Published by Iranian Aerospace Society This article is an open access article distributed under the terms and conditions of the Creative Commons Attribution 4.0 International (CC BY 4.0)

<https://creativecommons.org/licenses/by/4.0/>.



HOW TO CITE THIS ARTICLE:

Sevda Rezazadeh Movahhed, Mohammad Ali Hamed "Aerodynamic Coefficients Computation for Fixed Wing Aircrafts Using DATCOM Software with Emphasis on Rudderless Flying-Wing UAVs", *Journal of Aerospace Science and Technology*, Vol 17, No1,2024, pp, 60-71

DOI: [10.22034/jast.2023.398894.1152](https://doi.org/10.22034/jast.2023.398894.1152)

URL: https://jast.ias.ir/article_184299.html